

pairing switched off. In these CHF results, which are enumerated in Table I, we see no signs of a backbend and indeed this is consistent with the earlier CHF results^{12,13} for ²⁰Ne and ⁵⁶Ni.

We wish to emphasize that our results are not in contradiction to the basic idea of the alignment model.^{3,14} At the two critical J values a pair of neutrons and a pair of protons do align. But the antipairing continues to be operative and at two other values of J , larger than these J_c , complete disappearance of both neutron and proton pairings occurs. The alignment model does not describe the latter phenomenon. Amongst all the known methods and models for backbending, the CHFB seems to be the only one capable of describing all the stages in the transition from the paired (BCS) to the completely unpaired state for such large angular momentum values as in the second backbend region. Here we should also point out that within the CHFB framework one can equally well understand the lack of backends at relatively low J values in many of the odd A rotors. Since the CHFB allows for alignment, blocking to alignment (as it does in the alignment model¹⁴), can also take place. This has been demonstrated by Ring, Mang, and Banarjee.¹⁵ Thus all the existing data and the results reported here and elsewhere^{1,2} support the antipairing interpretation. If more than two backbends are ever seen in any rare-earth rotor, a significant modification in the above interpretation would become a necessity.

In view of our results, it would be very interesting to clear up the experimental uncertainty regarding the order of 843- and 855-keV transitions in ¹⁵⁸Er and thus decide whether it is a discontinuity or a small backbend.

It is in the demonstration of the importance of the pairing degree of freedom and, thus, in the identification of the basic reason for backbends

that we differ from Faessler and Ploszajczak.¹⁶

We thank the staff of the Computer Centre of Madras Indian Institute of Technology for their excellent help. One of us (S.C.K.N.) acknowledges with thanks the financial support from the Department of Atomic Energy, Government of India through Research Grant No. BRNS/24/74-77.

^(a)Present address: Institut für Kernphysik, Kernforschungsanlage, Jülich, West Germany.

¹H. J. Mang, Phys. Rep. **18C**, 325 (1975), and references therein.

²A. Ansari and S. C. K. Nair, Nucl. Phys. **A283**, 326 (1977).

³F. S. Stephens and R. S. Simon, Nucl. Phys. **A183**, 157 (1972).

⁴A. Faessler, K. R. Sandhya Devi, F. Grummer, K. W. Schmid, and R. S. Hilton, Nucl. Phys. **A256**, 106 (1976).

⁵B. R. Mottelson and J. G. Valatin, Phys. Rev. Lett. **5**, 511 (1960).

⁶T. Y. Lee, M. M. Aleonard, M. A. Deleplanque, Y. El-Masri, J. O. Newton, R. S. Simon, R. M. Diamond, and F. S. Stephens, Phys. Rev. Lett. **38**, 1454 (1977).

⁷M. K. Pal, unpublished.

⁸A. L. Goodman, Nucl. Phys. **A230**, 466 (1974).

⁹M. Baranger and K. Kumar, Nucl. Phys. **A110**, 490 (1968).

¹⁰F. Grummer, K. W. Schmid, and A. Faessler, Nucl. Phys. **A239**, 289 (1975).

¹¹A. P. Stamp, Nucl. Phys. **A161**, 81 (1971).

¹²S. K. Sharma, L. Satpathy, S. B. Khadkiker, and S. C. K. Nair, Phys. Lett. **61B**, 122 (1976).

¹³K. H. Passler and U. Mosel, Nucl. Phys. **A257**, 242 (1976).

¹⁴F. S. Stephens, Rev. Mod. Phys. **47**, 43 (1975).

¹⁵P. Ring, H. J. Mang, and B. Banarjee, Nucl. Phys. **A225**, 141 (1974).

¹⁶A. Faessler and M. Ploszajczak, Phys. Lett. **76B**, 1 (1978).

Description of the Polarization of ¹²B Produced in the Reaction ¹⁰⁰Mo(¹⁴N, ¹²B)¹⁰²Ru

T. Udagawa and T. Tamura

Department of Physics, The University of Texas, Austin, Texas 78712

(Received 2 August 1978)

The polarization of ¹²B produced in the reaction ¹⁰⁰Mo(¹⁴N, ¹²B)¹⁰²Ru is explained in a fully quantum mechanical way. It is found that recoil plays a decisive role.

Recently we applied successfully a multistep direct reaction (MSDR) theory to explain continuous spectra of reactions induced by both light⁵

and heavy⁶ ions. The most important ingredient in making such calculations possible was to recognize that, in calculating continuous cross sec-

tions, it is legitimate to replace realistic nuclear (final) states by members of an appropriately chosen complete set.⁵ It may also be emphasized that in applying our approach to heavy-ion reactions, it is practical and well justified⁶ to use a parametrized form of the distorted-wave Born-approximation (DWBA) amplitude.⁷ In the present article we apply the techniques developed in Refs. 5 and 6 to explain the data of Ref. 1. As is seen, the actual calculation was done within the one-step DR theory.

We first give a few formulas necessary in explaining some details of the calculations. Several of these formulas, and also part of the technique we use, were also used in a recent work by Bond.⁸ A major difference is that Bond considered only discrete final states, while we consider continuum states. Also, Bond's arguments remained largely speculative, with no attempt to fit existing data quantitatively.

The usual one-step (DWBA) amplitude may be written (with notation as in Tamura⁹) as

$$T_{I_B M_B s_b m_b}^{l m} = \langle I_B M_B s_b m_b | l m \rangle \beta_{l m}(\theta), \quad \beta_{l m}(\theta) = \sum_{l_a l_b} \langle l_a 0 l_b m | l m \rangle \hat{I}_{l_b l_a} (4\pi)^{1/2} (-1)^{l_b - m} Y_{l_b - m}(\theta, 0). \quad (1)$$

Note that Eq. (1) is simpler than the more general form of T given in Ref. 9. Here we have already assumed that the projectile has spin $s_a = 0$. Actually ^{14}N has $s_a = 1$, but the ($^{14}\text{N}, ^{12}\text{B}$) reaction proceeds primarily¹⁰ by letting two protons carry away two units of angular momenta from ^{14}N . This fact justifies the use of Eq. (1) so long as we set $s_b = 2$ (rather than $=1$, the spin of ^{12}B), and makes our discussion much more transparent than otherwise.

In Eq. (1), the coordinate system used has $\hat{z} \parallel \vec{k}_a$ and $\hat{y} \parallel \vec{k}_a \times \vec{k}_b$, where \vec{k}_a (\vec{k}_b) is the relative momentum in the incident (exit) channel. We found, however, that a new coordinate system,¹¹ in which $\hat{z} \parallel \vec{k}_a \times \vec{k}_b$ and $\hat{x} \parallel \vec{k}_a$, is more convenient to use for our purpose. We then have, in place of (1),

$$T_{I_B \lambda_B s_b \lambda_b} = \sum_{l \lambda} \langle I_B \lambda_B s_b \lambda_b | l \lambda \rangle \beta_{l \lambda}(\theta), \quad (2)$$

$$\beta_{l \lambda}(\theta) = \sum_m D_{m \lambda}^l(\frac{1}{2}\pi, \frac{1}{2}\pi, \pi) \beta_{l m}(\theta).$$

Clearly, λ , λ_B , and λ_b are projections, respectively, of l , I_B , and s_b along this new z axis.

As in Ref. 6, we parametrize the amplitude $I_{l_b l_a}$ in the form

$$I_{l_b l_a} = N_0 \exp\{-[(l_b - l_b^{(0)})^2 / \Gamma_b^2 + (l_a - l_a^{(0)})^2 / \Gamma_a^2] + i\psi(l_b - l_b^{(0)})\} \quad (\text{with } l_a = l_b - l_a). \quad (3)$$

We performed exact finite-range (EFR) DWBA calculations of $I_{l_b l_a}(\theta)$ for the reactions $^{100}\text{Mo}(^{14}\text{N}, ^{12}\text{B})^{102}\text{Ru}$ for about 3000 sets of the values of l_b , l , l_a , and E_b , and the parameters that appear in (3) were fixed so that these EFR-DWBA results are best reproduced in the sense of χ^2 . The values thus were $l_b^{(0)} = 55.7 + 0.61Q$, $l_a^{(0)} = 1.7 + 0.61Q$, $\Gamma_b = 4$, $\Gamma_a = 7$, and $\psi = 0.15$, the reaction Q value being measured in MeV.¹² Note that there appear in (3) two windows at $l_b^{(0)}$ and $l_a^{(0)}$, respectively, for the angular momenta l_b and l_a , with widths (4 and 7) which are fairly small compared with the maximum value of l_b which is of the order of 50. Note that N_0 is a real quantity depending slightly on l and other quantum numbers. We ignore this dependence, however, since it is not crucial to the discussion given below.¹³

In the above EFR-DWBA calculations, an optical potential with $V = 100$ MeV and $W = 10$ MeV, and $r_v = r_w = 1.3$ fm and $a_v = a_w = 0.5$ fm, was used. The form factor constructed for the ground-state transition was used throughout.

In Ref. 6, a straightforward use of (3) was made, and we can do so here too. In order to make the mechanism of polarization as transparent as possible, however, we shall go one step further in simplification, and use the following approximate relations¹¹:

$$(l_a 0 l_b m | l m) \approx (\hat{l} / \hat{l}_b) (-1)^{l+l_b} D_{m, l_a}^l(0, \frac{1}{2}\pi, 0), \quad (4)$$

$$Y_{l_b - m}(\theta, 0) \approx i^{m-|m|} (\pi \sin^{1/2}\theta)^{-1} \cos[(l_b + \frac{1}{2})\theta - \frac{1}{4}\pi - \frac{1}{2}|m|\pi].$$

We insert (1), (3), and (4) into (2) which has a double summation over l_a and l_b . The summation over l_a is replaced by one over l_a , which can be carried out analytically, by using the orthornormality of the D functions.¹¹ The summation over l_b is then replaced by an integral, which can also be performed

analytically. The result is

$$\beta_{i\lambda} = A(\theta) \hat{l}(-1)^{l+\lambda} [\beta_{i\lambda}^{(+)} + (-1)^l \beta_{i\lambda}^{(-)}], \quad A(\theta) = \Gamma_b / (4\pi \sin\theta)^{1/2}, \quad (5)$$

$$\beta_{i\lambda}^{(\pm)} = N_0 \exp\left\{ -(\lambda \mp l_d^{(0)})^2 / [\Gamma_d^2 + \frac{1}{4}\Gamma_b^2(\theta \mp \psi)^2] \mp i(l_b^{(0)}\theta + \frac{1}{2}\pi) \right\}.$$

The amplitudes $\beta_{i\lambda}^{(+)}$ and $\beta_{i\lambda}^{(-)}$, characterized by the deflection angles ψ and $-\psi$, respectively, describe contributions coming from processes taking place on near and far sides of the nucleus. Since $\psi > 0$ in our case, $\beta_{i\lambda}^{(+)}$ dominates $\beta_{i\lambda}^{(-)}$, although the contribution of the latter is not necessarily negligible.

Comparison of (5) with (3) shows that the l_d -space window in the latter has resulted in a window in the λ space, located at $\lambda = \pm l_d^{(0)}$ for $\beta_{i\lambda}^{(\pm)}$. The value of $l_d^{(0)} = 1.7 + 0.61Q$, as given above, is negative for all the Q values concerned; $Q < Q_g$, where $Q_g = -7.5$ MeV is the Q value for the ground-state transition. Therefore, negative $\lambda \approx l_d^{(0)}$ (positive $\lambda \approx -l_d^{(0)}$) contribute dominantly to $\beta_{i\lambda}^{(+)}$ ($\beta_{i\lambda}^{(-)}$).

In terms of $\beta_{i\lambda}^{(\pm)}$, the cross section and the polarization of ^{12}B for exciting a single state in ^{102}Ru with a spin I_B and excitation energy E_B^* ($=Q_{g.s.} - Q$) are written as

$$\sigma(I_B E_B^*, \theta) = \sum_{i\lambda} |\beta_{i\lambda}|^2 = |A(\theta)|^2 \sum_{i\lambda} (2l+1) |\beta_{i\lambda}^{(+)} + (-1)^l \beta_{i\lambda}^{(-)}|^2, \quad (6a)$$

$$P(I_B E_B^*, \theta) \sigma(I_B E_B^*, \theta) = \sum_{i\lambda} [(s_b + 1)/s_b]^{1/2} (l' \lambda 10 | l \lambda) \hat{l}' \hat{s}_b W(1s_b I_B; s_b l') \beta_{i\lambda} \beta_{i\lambda}^*. \quad (6b)$$

The continuum spectra are then obtained as

$$d\sigma/dE_b = \sum_{I_B} \sigma(I_B E_B^*, \theta) \rho(I_B E_B^*) \quad \text{and} \quad P(E_B^*, \theta) d\sigma/dE_b = \sum_{I_B} P(I_B E_B^*, \theta) \sigma(I_B E_B^*, \theta) \rho(I_B E_B^*). \quad (7)$$

Here $\rho(I_B E_B^*)$ is the spectroscopic density,^{5,6} and was constructed by using the method described in some detail in the second paper of Ref. 5. As can be seen there, this $\rho(I_B E_B^*)$ is very close to the level density with which two protons occupy a pair of vacant orbits in a shell model.

Numerical calculations were performed based on the formulas given above, and the results are presented in Fig. 1 with solid lines. It is seen that they agree rather well with experiment, although some deviation is noticed in the region of very small E_b , to which we will come back later.

The nice agreement obtained encourages us to go one step further into a deeper understanding of how the above results came about. For this purpose, we shall first put $s_b = 2$ in (6b), and then express explicitly the Racah and Clebsch-Gordan coefficients that appear there. If we write $P = P_1 + P_2$, the result is given as

$$\sigma P_1 = |A|^2 \sum_{i\lambda} \frac{(2l+1)}{4l(l+1)} \lambda [6 + l(l+1) - I_B(I_B+1)] |\beta_{i\lambda}^{(+)} + \beta_{i\lambda}^{(-)}|^2, \quad (8a)$$

$$\sigma P_2 = |A|^2 \sum_{\substack{i\lambda \\ (i \neq 0)}} \frac{(l^2 - \lambda^2)^{1/2}}{2l} [(I_B + l + 3)(I_B - l + 3)(I_B + l - 2)(l - I_B + 2)]^{1/2} [\beta_{l-1, \lambda}^{(+)} \beta_{i\lambda}^{(+)*} - \beta_{l-1, \lambda}^{(-)} \beta_{i\lambda}^{(-)*}]. \quad (8b)$$

The P_1 originates from the $l' = 1$ term in (6b), and the P_2 from the $l' = l \pm 1$ term. Note that P_2 in the form of (8b) is real, because the phase of $\beta_{i\lambda}^{(\pm)}$ is independent of l , as seen in (5).

We first want to obtain the asymptotic behavior of P_1 and P_2 . For simplicity, we set for the moment $\beta_{i\lambda}^{(-)} = 0$, since its magnitude is small compared with that of $\beta_{i\lambda}^{(+)}$. We have seen above that $\beta_{i\lambda}^{(+)}$ has a λ window at $\lambda = l_d^{(0)} < 0$, and that $|l_d^{(0)}|$ increases linearly with $|Q|$. As $|Q|$ increases, states with larger I_B become available, which allows l to be also large, since $\bar{I} = \bar{I}_B + \bar{2}$. However, the maximum possible value, L , of l increases only in proportion to $|Q|^{1/2}$ (as expected from the spin dependence of the level density). We thus have $L < |l_d^{(0)}|$ for a large $|Q|$, and this

fact leaves the factor $\exp[-(|\lambda| - |l_d^{(0)}|)^2 / \Gamma_d^2]$ in $\beta_{i\lambda}^{(+)}$ sufficiently large, only if $|\lambda|$ takes its largest possible value, i.e., if $|\lambda| = L$. This also requires that $l = L$. In other words, only one term with $l = -\lambda = L$ dominates the double sum in (8), and we arrive at the asymptotic relations by taking the limit $L = I_B + 2$ as

$$\sigma P_1 \xrightarrow{|Q| \rightarrow \infty} |A|^2 (-2L) (\beta_{L, -L}^{(+)})^2, \quad (9)$$

$$\sigma P_2 \xrightarrow{|Q| \rightarrow \infty} |A|^2 (l^2 - \lambda^2)^{1/2} \beta_{L, -L}^{(+)} \beta_{L-1, -L}^{(+)*}.$$

[For P_2 we retained a small factor $(l^2 - \lambda^2)^{1/2}$ which of course vanishes if the limit $l = -\lambda = L$ is taken literally.] Applying a similar argument to

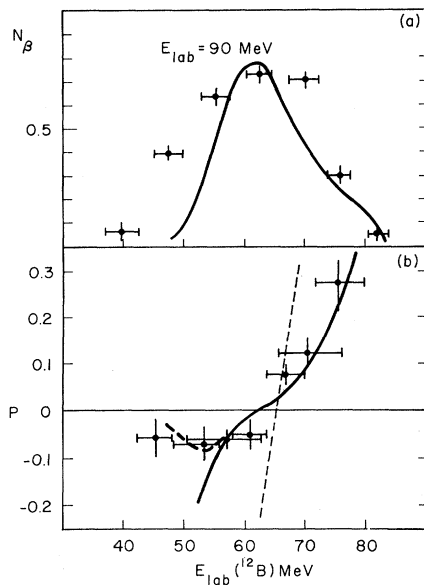


FIG. 1. (a) Number of observed β particles, N_β , which is proportional to the cross section, and (b) the polarization of ^{12}B , at $\theta_{\text{lab}}=20^\circ$. Experimental data were taken from Ref. 1. Prediction of Ref. 3 is given by dotted lines, while our prediction is given by solid and dashed lines. Theoretical cross section has been normalized at the peak of the N_β distribution.

(6a), we also get the asymptotic relation

$$\sigma \xrightarrow{|Q| \rightarrow \infty} |A|^2 (2L) (\beta_{L,-L}^{(+)})^2.$$

We thus have $P_1 \rightarrow -1$ and $P_2 \rightarrow 0$ as $|Q| \rightarrow \infty$.

As is clear from (8b), P_2 is positive definite (since $|\beta_{1\lambda}^{(+)}| > |\beta_{1\lambda}^{(-)}|$). It will have nonvanishing values for smaller $|Q|$, and tends to zero for large $|Q|$, as shown above. This behavior of P_2 is the same as that of the experimental P for large E_b , as is seen in Fig. 1.

In contrast to P_2 , P_1 is negative for all Q . To see this, we first note that the factor $6+l(l+1) - I_B(I_B+1)$ in (8a) changes its sign from negative to positive, as l is increased from I_B-2 to I_B+2 . On the average, however, this factor is positive. Since the other factor λ in (8a) is negative definite, it is seen that P_1 is indeed negative. For smaller $|Q|$, where only smaller I_B 's are available, the magnitude of P_1 will be small because the contributions from different l 's cancel one another, as a result of the varying sign of the above-mentioned factor. For large $|Q|$, $P_1 \rightarrow -1$, as shown above.

Summarizing, we found that for small $|Q|$, i.e., for large E_b , P_2 is dominant and explains by itself the experimental P there. For $E_b \approx 60$ MeV,

positive P_2 and negative P_1 compete and make $P \approx 0$. For E_b lower than 60 MeV, P_1 dominates, and tends to make P approach -1 . In this way the E_b dependence of the theoretical P is well understood.

It is now clear that, had we had $P_2=0$, we must have failed completely to fit the data. We reemphasize that P_2 results from the interference between amplitudes associated with l values that differ by one unit, i.e., with l 's that have opposite parities, natural and unnatural. It is well known (see, e.g., Ref. 9) that the amplitude associated with the unnatural-parity l vanishes identically if the DWBA calculation is made with no-recoil approximation. We then have $P_2=0$. The fact that we obtained nonvanishing P_2 was thus simply due to the fact that our calculation was based on EFR-DWBA, which takes fully into account the recoil effect. We can thus conclude that the appearance of large positive P in Fig. 1 is entirely due to the recoil effect.

We remarked above that $P \rightarrow P_1 \rightarrow -1$ for large $|Q|$, and this fact is going to make our theoretical P deviate from experiment for $E_b \lesssim 55$ MeV; see Fig. 1. We do not think this is a significant trouble in our theory, however. It should be noted that in the energy region with which we are concerned, we are also somewhat underpredicting the cross section, which we believe is because we have not included the contribution of higher-step processes.^{5,6} Postponing to a future work the inclusion of such effects in our calculation, we shall here simply assume that the discrepancy between the theoretical and experimental cross sections can be accounted for this way, and therefore that we can use the experimental, rather than the theoretical, cross section in the formula defining P in (7). (This assumes further that the higher-step processes are so complicated that their contributions to P average out to zero.) If this is done, we obtain a new theoretical result, shown in Fig. 1 by a dashed line, which is seen to be in good accord with experiment.

In the above discussions of the properties of P_1 and P_2 , we all but ignored the presence of the term $\beta_{1\lambda}^{(-)}$. From what we discussed below Eq. (5), however, it is clear that $\beta_{1\lambda}^{(-)}$ behaves in an almost opposite way to $\beta_{1\lambda}^{(+)}$. As we stated earlier, the condition that $\beta_{1\lambda}^{(-)}$ makes a significant contribution is that $\psi \leq 0$. Very recently, Takahashi *et al.*¹² repeated the experiment of Ref. 1, but with $E_{\text{lab}}(^{14}\text{N})=200$ MeV, and found that P became positive again for $-Q \geq 100$ MeV. It may be that ψ has indeed become negative, and thus

P_1 is contributing positively. Work to test such a conjecture is also under way.

We are very much indebted to the authors of Refs. 1 and 12, in particular to Professor K. Sugimoto, Professor H. Kamitsubo, and Dr. M. Ishihara, for a number of fruitful discussions. We also thank Professor K. Nagatani for stimulating conversations. Professor W. R. Coker read through the manuscript. This work has been supported in part by the U. S. Department of Energy.

¹K. Sugimoto, N. Takahashi, A. Mitzobuchi, Y. Nojiri, T. Minamisono, M. Ishihara, K. Tanaka, and H. Kamitsubo, *Phys. Rev. Lett.* **39**, 323 (1977).

²*Proceedings of the Third International Symposium on Polarization Phenomena in Nuclear Reactions, Madison, Wisconsin, 1970*, edited by H. H. Barschall and W. Haerberli (Univ. of Wisconsin Press, Madison, Wis., 1971), p. 3.

³M. Ishihara, K. Tanaka, K. Kammuri, K. Matsuoka, and M. Sano, *Phys. Lett.* **73B**, 281 (1978).

⁴D. M. Brink, *Phys. Lett.* **40B**, 37 (1972).

⁵T. Tamura, T. Udagawa, D. H. Feng, and K. K. Kan, *Phys. Lett.* **66B**, 109 (1977); T. Tamura and T. Udagawa,

Phys. Lett. **71B**, 273 (1977).

⁶T. Udagawa, B. T. Kim, and T. Tamura, in *Proceedings of the IPCR (Institute of Physical and Chemical Research) Symposium, Hakone, Japan, September 1977*, edited by H. Kamitsubo and M. Ishihara (unpublished), p. 3.

⁷V. M. Strutinsky, *Zh. Eksp. Teor. Fiz.* **46**, 2078 (1964) [*Sov. Phys. JETP* **19**, 1401 (1964)]; S. Kahana, P. D. Bond, and C. Chasman, *Phys. Lett.* **50B**, 199 (1974).

⁸P. D. Bond, *Phys. Rev. Lett.* **40**, 501 (1978).

⁹T. Tamura, *Phys. Rep.* **14C**, 59 (1974).

¹⁰S. Cohen and D. Kurath, *Nucl. Phys.* **A101**, 1 (1967).

¹¹W. F. Frahn, *Nucl. Phys.* **A272**, 413 (1976).

¹²Precisely speaking Γ_b , Γ_d , and ψ all depend on the Q value. This dependence is rather weak, however, and this is neglected in the present calculations for simplicity.

¹³In principle N_0 may differ greatly for normal and non-normal l 's, particularly if the energy of the incident particle is low. With energy of the present reaction the dependence of N_0 on l , whether normal or non-normal, turned out to be very weak and we used a common value for all of them.

¹⁴N. Takahashi, Y. Miyake, Y. Nojiri, T. Minamisono, A. Mizobuchi, M. Ishihara, and K. Sugimoto, to be published.

Gamma-Ray Circular Polarization and Nuclear Spin Orientation in ^{16}O on Ni Reactions at 100 MeV

C. Lauterbach, W. Dünnweber, G. Graw, W. Hering, H. Puchta, and W. Trautmann

Sektion Physik, Universität München, D-8046 Garching, West Germany.

(Received 5 July 1978)

The circular polarization of the energy-integrated γ -ray spectra and the angular correlation of discrete γ transitions in coincidence with the light fragments detected at 35° were measured for the reaction 100-MeV $^{16}\text{O} + \text{Ni}$. A large nuclear spin polarization and at least 80% negative-angle scattering are deduced for deep-inelastic events. The decrease of the circular polarization observed at $Q > -30$ MeV is ascribed to increasing positive-angle contributions to the cross section.

It has been shown that the γ radiation emitted by the excited fragments of deep-inelastic (DI) heavy-ion reactions is circularly polarized and that the sense of rotation of the intermediate complex formed by the colliding nuclei can be determined.¹ In the case of 300-MeV ^{40}Ar on Ag a polarization in the direction of the scattering normal $\vec{k}_i \times \vec{k}_f$ was found which established the predominance of orbiting trajectories leading to negative classical deflection angles. The measured value of about 25% γ -ray circular polarization seems to be rather small, however, since large spin alignment has been observed for the highly excited primary fragments of DI reactions.²⁻⁴ This alignment is interpreted as resulting from the transfer of a considerable part of the orbital

angular momentum into intrinsic fragment spins due to tangential friction. A large nuclear spin polarization is therefore expected which should lead to a large γ -ray circular polarization if most of the spin is carried away in cascades of stretched γ transitions.

In general, a γ -ray circular polarization of less than 100% will be found if (i) nonstretched transitions take part in the γ -decay process, if (ii) nonaligned spin is generated either in the primary collision or by the emission of light particles, if (iii) processes with positive and negative scattering angles contribute to the observed cross section (which does not exclude a large alignment), or if (iv) the two fragments emerge with opposite spin directions^{5,6} and emit γ radiation of